Impact of Wave Dragon on Wave Climate

Andersen, Thomas Lykke; Tedd, James; Kramer, Morten; Kofoed, Jens Peter

Publication date:
2006

Document Version
Publisher's PDF, also known as Version of record

AALBORG UNIVERSITY

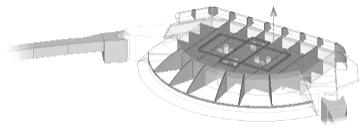

Impact of Wave Dragon on Wave Climate

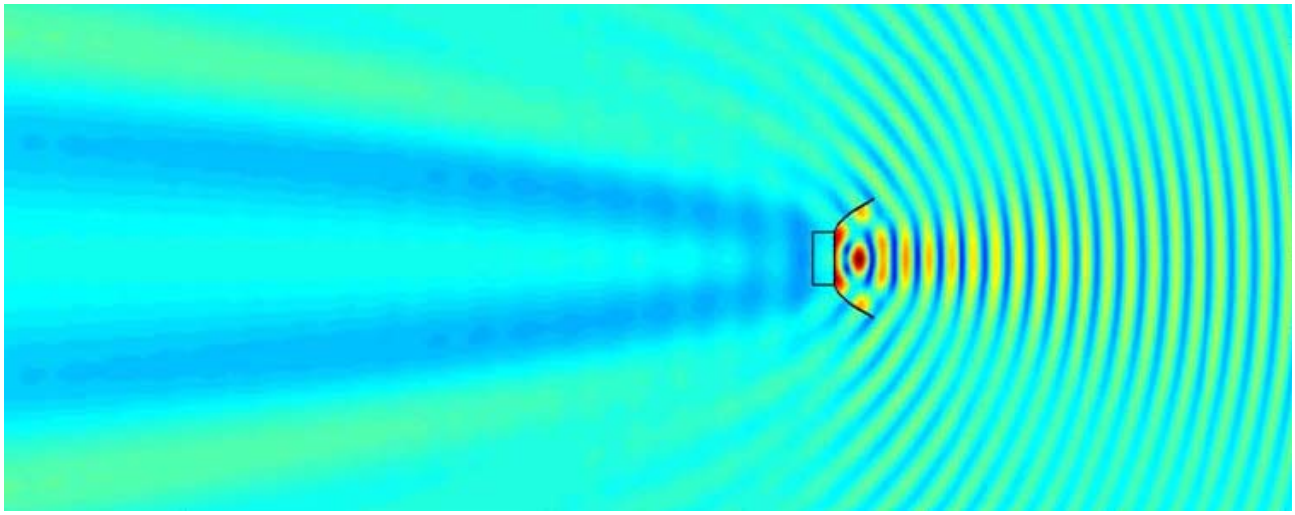

Thomas Lykke Andersen, James Tedd, Morten Kramer & Jens Peter Kofoed
Aalborg University

April, 2006

Department of Civil Engineering
Aalborg University - Sohngaardsholmsvej 57 - DK 9000 Aalborg - Telephone +45 9635 8080

DEPARTMENT OF CIVIL ENGINEERING
AALBORG UNIVERSITY
SOHNGAARDSHOLMSVEJ 57 DK-9000 AALBORG DENMARK
TELEPHONE +45 96 35 80 80 TELEFAX +45 98 14 25 55

Hydraulics and Coastal Engineering No. 42

ISSN: 1603-9874

Impact of Wave Dragon on Wave Climate

by

Thomas Lykke Andersen, James Tedd, Morten Kramer & Jens Peter Kofoed
Aalborg University

April, 2006

Content

1. Preface

This report is an advisory paper for use in determining the wave dragon effects on hydrography, by considering the effect on the wave climate in the region of a wave dragon. This is to be used in the impact assessment for the Wave Dragon pre-commercial demonstrator

For further information please contact:

James Tedd

Marie Curie WaveTrain RTN fellow and Research Assistant

Aalborg University,

Department of Civil Engineering,

Hydraulics and Coastal Engineering Laboratory,

Sohngaardsholmsvej 57,

DK-9000 Aalborg, Denmark.

Room: C.212

Phone: (+45) 96 35 84 74/(+45) 27 22 42 88

Fax: (+45) 98 14 25 55

E-mail: i5jt@civil.aau.dk

2. Introduction

A potential flow solution based on the boundary element method (BEM) is used to estimate the effect of the Wave Dragon on the wave field in the region of the wave dragon. This method presents the relative wave amplitude for the cases of regular waves in the operational region of the Wave Dragon device.

These wave fields are to be used to examine the effect of the Wave Dragon on the wave climate, coastal processes and other fields behind the device.

3. Model theory

The program ShipBEM developed at Aalborg University is used for the calculations. This program is based on a 3D boundary element method (BEM). The model BEM code used is the same as applied by Kramer, M. and Frigaard, P. (2005) to estimate the effect of adding arms to a wave energy converter. Kramer, M. and Frigaard, P. (2005) showed very good correlation between numerical and small scale physical model tests for this model.

In BEM the meshing requirement is reduced to the structure's boundary surface. As a result it provides an efficient and accurate frequency domain solution for linear wave structure interaction problems. A source/sink distribution technique (Wehausen & Laitone, 1960) based on potential flow theory is used to calculate the velocity potentials φ in the Laplace equation. In the following the main procedure in the calculations is given.

In potential flows we can use the Laplace equation:

$$\nabla^2\varphi = 0 \qquad ,\nabla^2 = \left(\frac{\partial^2}{\partial x^2},\frac{\partial^2}{\partial y^2},\frac{\partial^2}{\partial z^2}\right) \tag{1}$$

The water depth is constant and the incoming waves are regular first order waves. Therefore the total wave field can be calculated by superposition.

$$\varphi = \varphi_0 + \varphi_s \tag{2}$$

φ_0 is the potential in the undisturbed incoming wave and φ_s is the scattered disturbance due to the presence of the Wave Dragon. Both φ_0 and φ_s satisfies the Laplace equation. The solution to φ_0 is:

$$\varphi_0 = \frac{ag}{\omega}\frac{\cosh k(z+h)}{\cosh kh}\cos(\omega t - kx) \tag{3}$$

ω is circular wave frequency, g is acceleration of gravity, t is time, a is wave amplitude, h is water depth and x the position. The wave number k is found from the dispersion relation.

$$\frac{\omega^2}{g} = k\tanh kh \tag{4}$$

The boundary conditions (BC) for φ_s on the water surface, i.e. the kinematic BC (a particle stays on the surface) and the dynamic BC (p=0 in the Bernoulli equation) can be written.

$$\frac{\partial^2\varphi_s}{\partial t^2} + g\frac{\partial\varphi_s}{\partial z} = 0 \quad \text{, on } z=0 \tag{5}$$

At the sea bed no water can flow through the bed, i.e.

$$\frac{\partial\varphi_s}{\partial n} = 0 \quad , \quad z=-h \tag{6}$$

In Eq. 6 n is the normal to the sea bed. At the fixed reflector boundary surface S_L the following condition must be fulfilled.

$$\frac{\partial \varphi_s}{\partial n} = -\frac{\partial \varphi_0}{\partial n} \quad \text{, on } S_L \tag{7}$$

Because the Laplace equation is an elliptic equation the BC's must be given along the whole boundary. At the vertical boundary Sommerfelds radiation condition are used.

$$\frac{\partial \varphi_s}{\partial r} + \frac{1}{c_w}\frac{\partial \varphi_s}{\partial t} = 0 \text{ , for } r \to \infty \tag{8}$$

In Eq. 8 c_w is the velocity of wave propagation.

As shown by Wehausen and Laitone (1960) it is possible to construct the function $A_E(x,\xi)$ in Eq. 9 in such a way that the boundary conditions at sea bed, water surface and radiation boundary all are fulfilled. This for a pulsating point source.

$$\varphi_{one\ source} = f\, A_E(x,\xi)\cos(\delta - \omega t) \tag{9}$$

Where f is source strength, δ is source phase, x is observation point and ξ is position of source. The expression for A_E will not be repeated in this paper.

The reflector surface is discretized into elements with sources distributed over each facet element. In the present calculations a constant source strength distribution is used for each element. The potential for one element is calculated by integration over the element surface:

$$\varphi_{one\ element} = \iint_{S_L} f\, A_E(x,\xi)\cos(\delta - \omega t)\, dS_L \tag{10}$$

Where S_L is the panel surface.

The individual panels are given index j and the potential in an observation point is calculated by superposition of the N panel-sources:

$$\varphi_s = \sum_{j=1}^{N} \varphi_j \tag{11}$$

The numerical task is therefore reduced to calculate f_j and δ_j with respect to the surface boundary condition (Eq. 7). This is done at two different times and $2N$ linear equations for f_j and δ_j are established. How to establish those equations will not be repeated in this paper. When φ_s is known, φ is calculated by Eq. 2.

From the linearized dynamic free surface condition (Bernoulli equation) the complex amplitude η of the free surface oscillation is derived.

$$\eta(x,y,z) = -\frac{i\omega}{g}\varphi\,, \qquad z = 0 \tag{12}$$

where i is imaginary number.

4. Model Limitations

There are several limitations of this study:

No energy is absorbed in the simulation. In reality the waves are rushing up the ramp of Wave Dragons main body, and the main part of the wave energy is absorbed. However, this is assumed to have only minor influence on the wave field behind the wave dragon, as this energy escapes out of the domain. In front of the main body the waves are higher than in reality.

There is no motion of either the arms or main body of the wave dragon. This is assumed to have small influence of the wave field behind the wave dragon.

Long-crested regular waves are used. As the weather-vaning action of Wave Dragon will make it face the predominant wave direction only head-on waves are tested. A real sea consists of a spectrum of waves approaching from a spread of directions. This study shows which wave frequencies are most affected by the device. The wave field behind the wave dragon is expected to be less disturbed for short-crested waves.

The Sea-bed is assumed to be smooth and horizontal – In reality there is energy lost in the boundary layer close to the seabed. This will cause a natural weakening of waves as they approach the shore.

It is felt that this study will enable a visualisation and a quantification of the effect of the Wave Dragon on the sea climate.

5. Model Meshing

The meshed model used has a total of 1110 panels. Due to a limit in the mesh plot software the model shown below is for a lower number of panels.

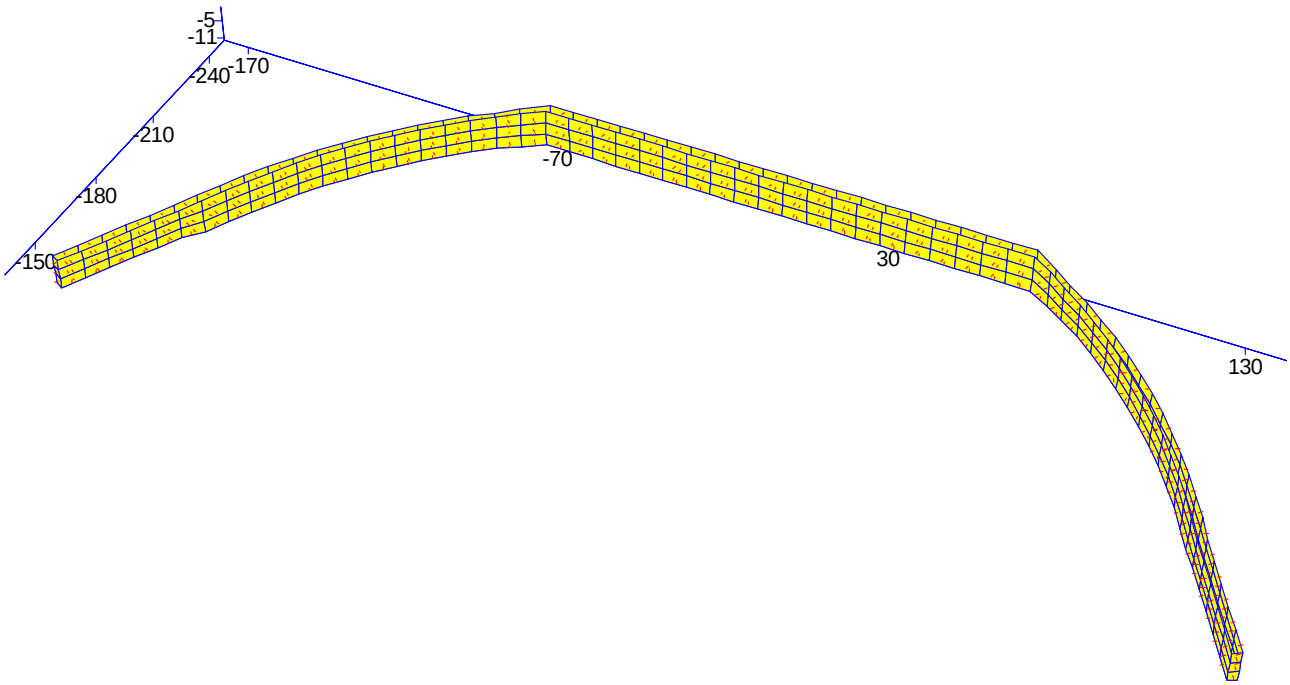

6. Results

In the present case regular first order waves are tested with periods in the region of those measured at the site north-west of Milford Haven (T = 11, 9, 7 and 5 s are tested). The depth of water used in these simulations is 37 m, and the sea-bed is considered to be smooth and horizontal.

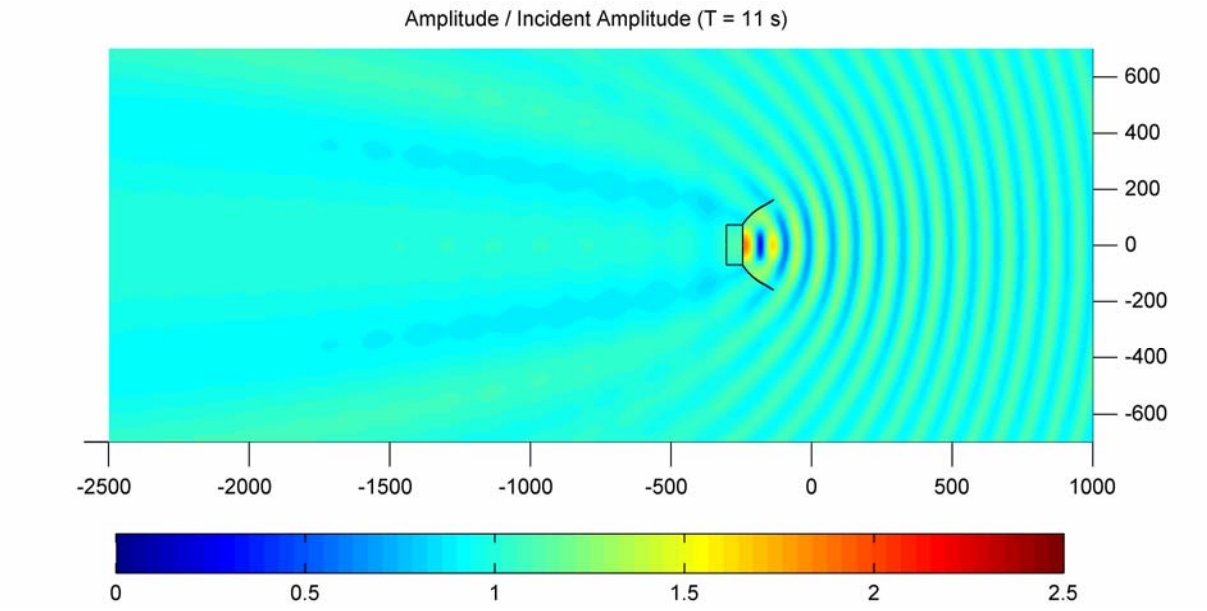

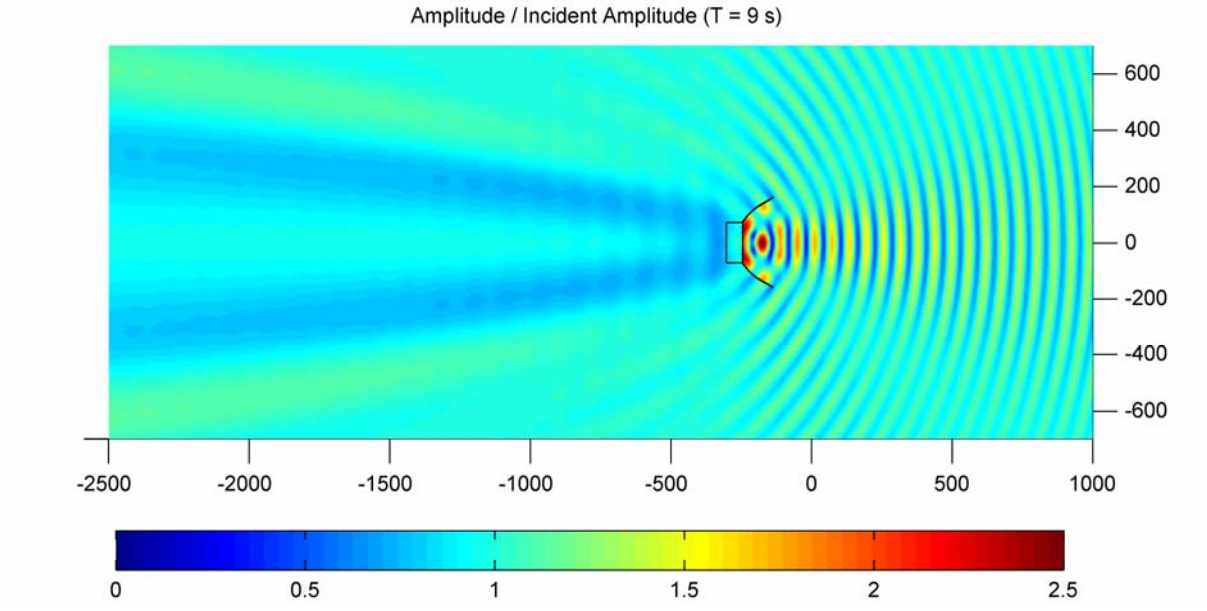

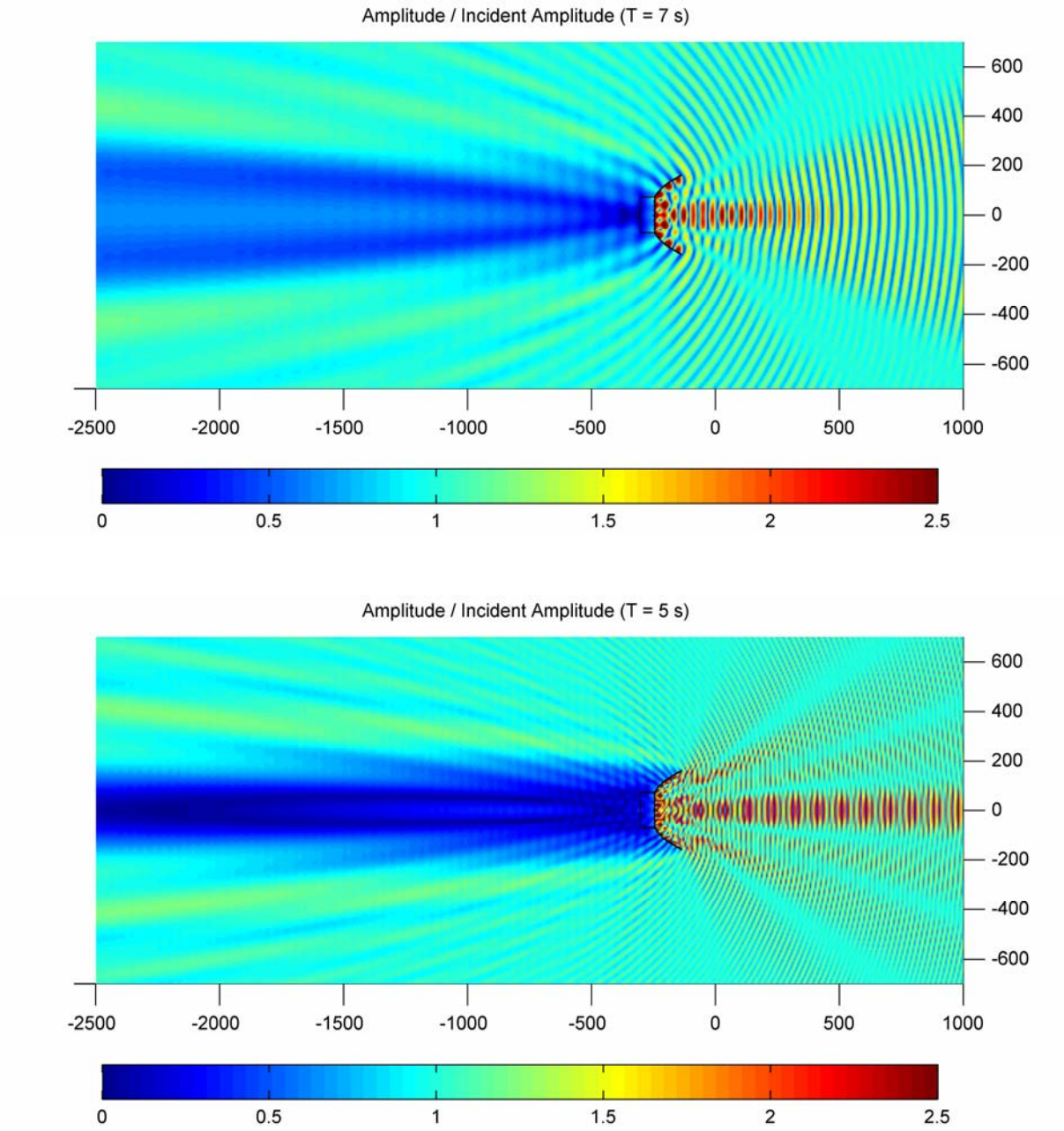

In front of the wave dragon the results show amplitudes larger than the amplitude of the incident waves. This is due to no energy absorption in the model and large energy absorption on the front side of the main body in reality. This reflected wave diffracts around the wave dragon. Behind the Wave Dragon the waves are smaller than the incident waves due to leeside effects. As expected this effect increases with decreasing wave period. This leads to wave field behind the wave dragon consisting of mainly the largest frequencies in the incident spectrum.

7. References

Kramer, M. and Frigaard, P. (2005). Reflectors to Focus Wave Energy. European Wave and Tidal energy Conference, 2005.